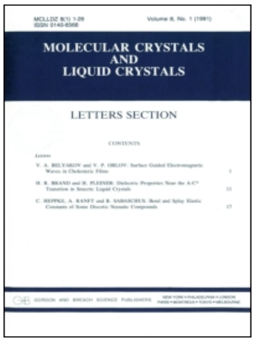

Molecular Crystals and Liquid Crystals

ISSN: 1542-1406 (Print) 1563-5287 (Online) Journal homepage: http://www.tandfonline.com/loi/gmcl20

Interaction of electromagnetic waves in nematic waveguide

M. F. Ledney, O. S. Tarnavskyy, A. I. Lesiuk & V. Yu. Reshetnyak

MOLECULAR CRYSTALS AND LIQUID CRYSTALS
2016, VOL. 638, 1–16
http://dx.doi.org/10.1080/15421406.2016.1217700

Taylor & Francis
Taylor & Francis Group

Interaction of electromagnetic waves in nematic waveguide

M. F. Ledney, O. S. Tarnavskyy, A. I. Lesiuk, and V. Yu. Reshetnyak

Faculty of Physics, Taras Shevchenko National University of Kyiv, Kyiv, Ukraine

ABSTRACT

Controlled by an electric field, the interaction of two coupled TE-modes at the dynamic grating in a planar waveguide with a thin layer of nematic liquid crystal has been studied theoretically. The dynamic grating is induced by an external electric field due to the periodicity of the anchoring energy of nematic with waveguide surface. Metal and dielectric waveguides have been studied. The transmission of TE-modes and its reflection from the periodic structure of the nematic layer have been investigated. The intensity of a signal- mode at the output of the waveguide has been calculated. The dependence of intensity on the anchoring energy amplitude and modulation period, dimensions of the nematic layer and an external electric field has been analyzed. It was shown that the frequency interval of a TE-mode reflection expands with increasing of the electric field. The primary maximum of the reflected mode intensity, as function of the nematic layer length, increases monotonously with growing s number of anchoring energy periods placed on the layer length. The primary peak reaches the largest value of 1 for $s \sim 10 \div 100$ (metal waveguide) and for $s \sim 1000$ (dielectric waveguide). The same dependence for the signal-mode, which propagates through the NLC layer, has nonmonotonous form and a complete energy exchange is reached only for certain values of s and the length of the nematic layer.

KEYWORDS

Nematic liquid crystal; liquid crystal waveguide; dynamic director grating; coupled modes; spatially periodic anchoring energy

Introduction

Over the last decades, the wide application of liquid crystals (LCs) in display technologies and high-tech electronic optical devices has evoked much interest to the processes of electromagnetic wave propagation in the liquid crystal cells, especially in nematic liquid crystals (NLCs) and NLC waveguides. In particular, the peculiarities of propagation and interaction of light beam modes in waveguides fully or partially filled with nematic liquid crystal (NLC) were studied in [1–8]. Functioning of wide range of integrated optical devices, such as optical filters and mode converters, distributed feedback lasers, frequency-selective optical couplers, Bragg reflection waveguides, are based on the interaction of electromagnetic waves and their modes in spatially periodic dielectric medium. Using easy-created by external electric/magnetic fields dynamic director grating makes the interaction of electromagnetic waves controllable and, therefore, proposes more opportunities for technological application of LC in the integrated optical devices. In particular, authors in [9] have experimentally investigated the energy exchange between *TM*-modes of the electromagnetic wave on the

CONTACT Mykhaylo F. Ledney Ledney@univ.kiev.ua Faculty of Physics, Taras Shevchenko National University of Kyiv, Prosp. Glushkova, 4, Kyiv, 03022, Ukraine.
Color versions of one or more of the figures in the article can be found online at www.tandfonline.com/gmcl.

director inhomogeneity, which is induced by the propagated wave, in the plane waveguide filled with NLC with a hybrid director orientation. The energy exchange between electromagnetic waves at director gratings which was induced by photorefraction in photoconducting LCs [10–12] and in LCs bounded by photorefractive polymer substrates [13–15] was studied as well. Also, the two-beam energy exchange was studied at director grating in hybrid cells of NLC with photorefractive substrates [16,17]. The interaction between coupled electromagnetic waves at a director grating induced by a change in potential difference was investigated in [18]. Such interaction was studied at a director grating induced by external light field [19] in a cell of NLC with photorefractive substrates. The theoretical model of a controllable by an electric field Bragg resonator, which is based on metal waveguide filled with NLC, is represented in [20].

The aim of our work is to study theoretically the energy exchange between two coupled modes of electromagnetic *TE*-waves at the director grating in a planar dielectric and metal waveguides with an NLC layer bounded in the direction of wave propagation. The grating is induced by an external low-frequency electric field due to periodicity of the NLC anchoring energy at the waveguide surface. The transmission and reflection of electromagnetic waves in the NLC layer of both dielectric and metal waveguides have been studied. Using the coupled modes approximation the intensity of a signal *TE*-mode at the output of the waveguide has been calculated and its dependence on the NLC layer parameters, the anchoring energy parameters and an external electric field has been investigated. The frequency interval of *TE*-mode reflection in the waveguide has been found, its dependence on an external electric field has been studied. The conditions for maximum signal-mode intensity in cases of reflection and transmission of an electromagnetic *TE*-mode through the NLC layer has been established. The results of the investigation could be taken in account in development and construction of new integrated optical devices.

Problem formulation and general equations used for its solution

We assume that an infinite planar waveguide is restricted by the same dielectric media in the region $|z| \leq L/2$. In the region $0 \leq y \leq D$ the waveguide is filled with NLC whose director initially has a uniform orientation along Ox axis. The NLC layer length D is assumed to be much greater than its thickness L. The waveguide is placed in an external uniform electric field whose intensity vector $\mathbf{E}_0$ is directed along Oz axis (see Fig. 1). The surface azimuthal anchoring energy of NLC is assumed to be infinitely large when the director is reoriented in the plane xOy. The polar anchoring energy induced by the director deviation in the plane xOz is assumed to be a periodic function of y and is taken in the form $W(y) = W_0 + V\cos(2\pi y/d)$, where $0 \leq V \leq W_0$. There exist different techniques for creating a spatially periodic NLC anchoring energy. In [21] linearly polarized light, which had passed through a periodic photomask, was incident on the surface treated with photopolymer. The spatial period of anchoring energy in that experiment was $d \sim 1 \div 10\ \mu$m. The anchoring energy can also be changed by varying the thickness of photopolymer [22] or by using a nanostructural alignment layer [23].

Flexopolarization is assumed to be absent and Frank-elastic constants we set to be equal(one constant approximation). For given geometry the Freedericksz transition, as shown in [24,25], takes xz-place. The geometry is assumed to be uniform along Ox axis. Accordingly, the director can be described as

$$\mathbf{n} = \mathbf{e}_x \cdot \cos\theta\left(y, z\right) + \mathbf{e}_z \cdot \sin\theta\left(y, z\right), \tag{1}$$

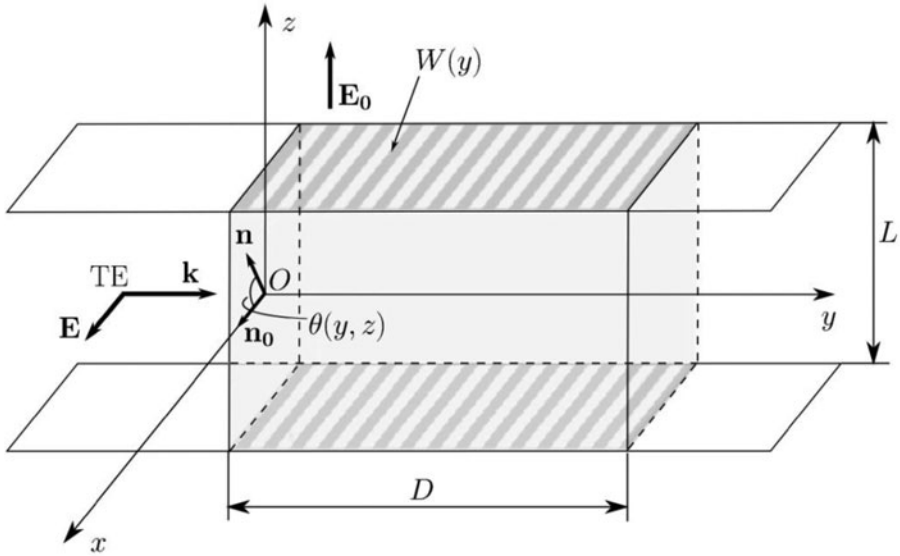

Figure 1. The geometry of the problem: D – the length of NLC layer, L – the waveguide thickness, $\mathbf{n}$ – the director of NLC, $\theta(z, y)$ – the angle of the NLC director $\mathbf{n}$ deviation out of its initial homogeneous direction $\mathbf{n}_0$, $\mathbf{E}_0$ - the low-frequency external electric field, $\mathbf{k}$ – the wave vector and $\mathbf{E}$ – an electric field of the *TE*-wave, $W(y) = W_0 + V\cos(2\pi y/D)$ – the polar azimuthal anchoring energy of NLC.

where $\theta(y, z)$ is the angle of deviation from the initially uniform director orientation along Ox axis, and $\mathbf{e}_x$ and $\mathbf{e}_z$ are the unit vectors of Cartesian coordinate system.

The free energy of NLC can be written as follows:

$$\begin{aligned}
F &= F_{el} + F_E + F_S,\\
F_{el} &= \frac{1}{2}\int_V \left\{K_1(\operatorname{div}\mathbf{n})^2 + K_2(\mathbf{n}\cdot\operatorname{rot}\mathbf{n})^2 + K_3[\mathbf{n}\times\operatorname{rot}\mathbf{n}]^2\right\} dV,\\
F_E &= -\frac{\varepsilon_a^0}{8\pi}\int_V (\mathbf{nE})^2\, dV,\\
F_S &= -\frac{1}{2}\int_S W(y)\,(\mathbf{ne})^2\, dS.
\end{aligned} \tag{2}$$

Here, F_{el} is the Frank elastic energy, F_E is anisotropic contribution to the free energy made by the electric field, F_S is the surface free energy taken in the form that generalizes Rapini's potential [26] for the case of non-uniform anchoring energy, $K_1,\ K_2,\ K_3$- Frank elastic constants, $\varepsilon_a^0 = \varepsilon_\parallel^0 - \varepsilon_\perp^0 > 0$ is the anisotropy of low-frequenc permittivity, $\mathbf{e}$ is the unit vector of director easy-orientation axis at the waveguide surface ($\mathbf{e} \parallel Ox$).

Minimizing the free energy (2) with respect to the angle θ by which the director $\mathbf{n}$ (1) deviates, in the one constant approximation $K_1 = K_2 = K_3 = K$ we obtain the following equation:

$$\frac{\partial^2\theta}{\partial y^2} + \frac{\partial^2\theta}{\partial z^2} + \frac{\varepsilon_a^0 E_z^2}{4\pi K}\sin\theta\,\cos\theta = 0 \tag{3}$$

and boundary conditions

$$\left[\pm K\frac{\partial\theta}{\partial z} + \left(W_0 + V\cos\frac{2\pi y}{d}\right)\sin\theta\cos\theta\right]_{z=\pm L/2} = 0. \tag{4}$$

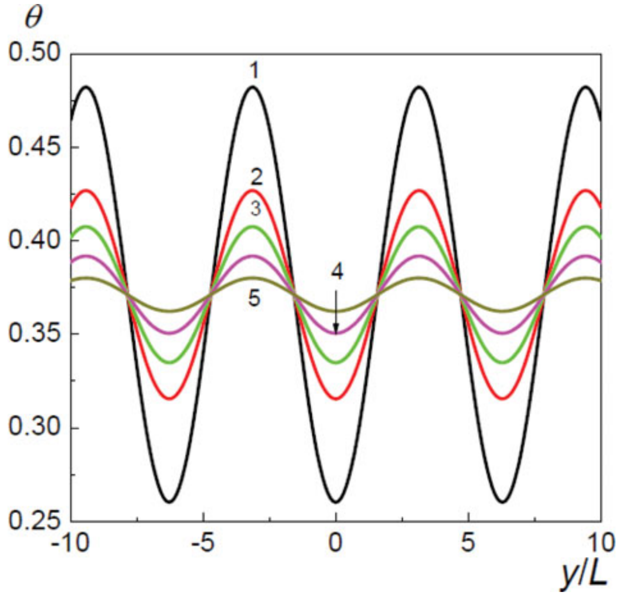

Figure 2. The dependence of the director deviation angle θ on the y at $z = 0$. $L/d = 0.16$ (1), 0.17 (2), 0.18 (3), 0.2 (4), 0.25 (5).

The equation for the director (3) and boundary conditions (4) should be considered together with Maxwell's equations for the electric field $\mathbf{E}$ in the volume of NLC. We neglect the boundary effects at NLC side surfaces and assume the angle θ to be a periodic function of y: $\theta(y + D, z) = \theta(y, z)$. Then the solution of the equation (3) could be found in the form of Fourier expansion in y.

Now we restrict ourselves to the case in which the number of anchoring energy periods d per NLC layer length D is an integer, i.e., the ratio $s = D/d$ is integer. If the electric field intensity $\mathbf{E}_0$ exceeds the Freedericksz transition threshold then a spatially periodic structure of nematic director is formed in the NLC layer along Oy axis. This grating appears due to periodicity of NLC surface anchoring energy in y. The period of the grating is equal to the period of the anchoring energy [24,25]. Therefore, when the intensity E_0 exceeds the threshold E_{0th} by a small value (parameter $\theta_m \ll 1$) in case the anchoring energy is large ($\xi = W_0 L/K \gg 1$) but slightly nonuniform, i.e., the anchoring energy modulation amplitude $\upsilon \ll \xi L^2/d^2$, the angle of nematic director deviation (1) can be described by expression [27]:

$$\theta\left(y, z\right) = \theta_m \cos\left(pz\right) - \frac{\upsilon pL\theta_m}{\xi \cos \lambda_s} \cos \frac{2\lambda_s z}{L} \cos \frac{2\pi y}{d}. \tag{5}$$

In this expression $E_{0th} = \frac{2\mu}{\pi} E_\infty (1 - \frac{\upsilon^2}{\xi})$, $E_\infty = \frac{\pi}{L}\sqrt{\frac{4\pi K}{\varepsilon_a^0}}$ is the Freedericksz transition threshold for the case of uniform infinite anchoring energy, μ is the smallest positive root of equation $\mu \tan \mu = \frac{\xi}{2}$, $\theta_m = \sqrt{\frac{4}{\gamma}\left(\frac{E_0}{E_{0th}} - 1\right)}$, $\upsilon = \frac{V}{W_0}$, $\gamma = 1 + \frac{3\varepsilon_a^0}{\varepsilon_\perp^0}$, $\lambda_s = \pi L\sqrt{\frac{p^2}{4\pi^2} - \frac{s^2}{D^2}}$, $p = \frac{\pi E_0}{LE_\infty}$.

The overthreshold spatial distribution of director in the middle of the NLC cell calculated by formula (5) for several values of L/d-ratio at the electric field values $E_0 = 1.05E_{0th}$ and $\xi = 100$, $\upsilon = 0.1$ is presented in Fig. 2. The general case of arbitrary values for parameter s and constituent part ξ of the anchoring energy has been comprehensively studied in [27].

We will assume now that in the waveguide with NLC layer whose director spatial distribution is described by expression (5), an electromagnetic TE-wave with frequency ω, which is polarized along Ox, propagates along the positive direction of the axis Oy (see Fig. 1). The intensity I of TE-wave is assumed to be so small that it does not change the spatial distribution of NLC director, $I \ll \frac{c\sqrt{\varepsilon_\parallel}\pi^2 K}{2\varepsilon_a L^2}$. Here $\varepsilon_a = \varepsilon_\parallel - \varepsilon_\perp$, $\varepsilon_\parallel$, $\varepsilon_\perp$- anisotropy of permittivity and eigenvalues of the electric permittivity tensor for homogeneous NLC at the frequency of an electromagnetic wave, respectively. Using NLC layer parameters $L = 10\ \mu$m, $K = 10$ dyn, $\varepsilon_\parallel = 2.9$, $\varepsilon_a = 0.5$ [28], which are near to typical ones, we obtain the criterion $I \ll 5 \cdot 10^4\ \mathrm{W/cm^2}$. We will further neglect the absorption of TE wave in both the NLC itself and surrounding dielectric medium, as well as the scattering of TE-wave by the director thermal fluctuations. The electric field $\mathbf{E} = (E_x, 0, E_z)$ of TE-wave in the bulk of NLC can be found from equation

$$\nabla\, \mathrm{div}\mathbf{E} - \Delta\mathbf{E} - \frac{\omega^2}{c^2}\hat{\varepsilon}\mathbf{E} = 0. \tag{6}$$

Here the NLC permittivity tensor $\hat{\varepsilon}$, given with the accuracy to the small terms of the order of θ_m^2, is a function modulated in the y-direction:

$$\hat{\varepsilon}\left(y, z\right) = \hat{\varepsilon}^0\ (z) + \Delta\hat{\varepsilon}\ (z) \cos\frac{2\pi y}{d},$$

$$\hat{\varepsilon}^0\ (z) = \begin{pmatrix} \varepsilon_\parallel - \varepsilon_a\theta_m^2\cos^2 pz & 0 & \varepsilon_a\theta_m\cos pz \\ 0 & \varepsilon_\perp & 0 \\ \varepsilon_a\theta_m\cos pz & 0 & \varepsilon_\perp + \varepsilon_a\theta_m^2\cos^2 pz \end{pmatrix},$$

$$\Delta\hat{\varepsilon}\ (z) = -\frac{\varepsilon_a \upsilon\, pL\theta_m}{\xi\ \cos\ \lambda_s}\cos\frac{2\lambda_s z}{L}\begin{pmatrix} -2\theta_m\cos pz & 0 & 1 \\ 0 & 0 & 0 \\ 1 & 0 & 2\theta_m\cos pz \end{pmatrix}. \tag{7}$$

Normal modes of dielectric waveguide

First we will find normal TE-modes in the waveguide with permittivity tensor $\hat{\varepsilon}^0(z)$ which is independent of y. We find the solution of equation (6) in the form

$$\mathbf{E}\left(y, z\right) = e^{iky}\,\mathbf{E}\,(z)\,. \tag{8}$$

The unknown amplitude $\mathbf{E}(z)$ of the electric field of a TE-wave will be further designated as $\mathbf{A}(z)$ inside ($|z| \leq L/2$) and $\mathbf{B}(z)$ outside ($|z| > L/2$) the NLC layer.

Now we consider the propagation of a TE-wave in the NLC layer, $|z| \leq L/2$. We assume the component E_z of the electric field of a TE-wave to be a quantity of the same order as θ_m. Then, using the approximation $L \gg \lambda$ in (6), the following system of differential equations is obtained for the components $A_x(z)$ and $A_z(z)$ of electric field amplitude in NLC with the accuracy as high as the small terms of the order of θ_m^2

$$A''_x + \left(k_\parallel^2 - k^2\right)\ A_x = -k_a^2\theta_m A_z\cos pz + k_a^2\theta_m^2 A_x\cos^2 pz,$$
$$A''_z + \left(k_\perp^2 - k^2\right)\ A_z = -k_a^2\theta_m A_x\cos pz, \tag{9}$$

where $k_\parallel = \frac{\omega}{c}\sqrt{\varepsilon_\parallel}$, $k_\perp = \frac{\omega}{c}\sqrt{\varepsilon_\perp}$, $k_a = \frac{\omega}{c}\sqrt{\varepsilon_a}$. Here and further on, the derivatives of $\mathbf{A}(z)$ with respect to argument z are denoted by primes.

Taking into account Maxwell's equations and the form (8) of a TE-wave electric field, we reduce the boundary conditions for the electric field on the NLC surface $z = \pm L/2$ to the conditions for the amplitude $\mathbf{A}(z)$:

$$[\pm A'_x + \varkappa A_x]_{z=\pm L/2} = 0,$$
$$\left[\varepsilon_a\theta_m \cos(pz) A_x + (\varepsilon_\perp - \varepsilon_d) A_z\right]_{z=\pm L/2} = 0, \tag{10}$$

where ε_d is the permittivity of medium surrounding NLC.

The electric field amplitude $\mathbf{A}(z)$ (and $\mathbf{B}(z)$ analogously) and the wave number k of a *TE*-wave (8) are found in the form of expansions in small parameter θ_m:

$$A_x(z) = A_{0x}(z) + A_{1x}(z)\,\theta_m + A_{2x}(z)\,\theta_m^2 + o\left(\theta_m^2\right),$$
$$A_z(z) = A_{1z}(z)\,\theta_m + A_{2z}(z)\,\theta_m^2 + o\left(\theta_m^2\right),$$
$$k = k_0 + k_1\theta_m + k_2\theta_m^2 + o\left(\theta_m^2\right). \tag{11}$$

Now we write the equations (9) and the boundary conditions (10) taking into account the expansions (11) with the accuracy up to the small terms of the order of θ_m^2. Assuming the coefficient at appropriate orders of θ_m to equal zero, we derive the following differential equations and corresponding boundary conditions from which the unknown functions $A_{0x}(z)$, $A_{1x}(z)$, $A_{2x}(z)$, $A_{1z}(z)$, $A_{2z}(z)$ as well as unknown parameters k_0, k_1, k_2 could be determined:

$$A''_{0x} + \alpha^2 A_{0x} = 0,$$
$$[\pm A'_{0x} + \varkappa_0 A_{0x}]_{z=\pm L/2} = 0, \tag{12}$$

$$A''_{1x} - 2k_1k_0A_{0x} + \alpha^2 A_{1x} = 0,$$
$$\left[\pm A'_{1x} + \varkappa_0 A_{1x} + \frac{k_0k_1}{\varkappa_0}A_{0x}\right]_{z=\pm L/2} = 0, \tag{13}$$

$$A''_{2x} + \alpha^2 A_{2x} = 2k_2k_0A_{0x} - k_a^2A_{1z}\cos pz + k_a^2A_{0x}\cos^2 pz,$$
$$\left[\pm A'_{2x} + \varkappa_0 A_{2x} + \frac{k_0k_2}{\varkappa_0}A_{0x}\right]_{z=\pm L/2} = 0, \tag{14}$$

$$A''_{1z} + \beta^2 A_{1z} = -k_a^2A_{0x}\cos pz,$$
$$[(\varepsilon_\perp - \varepsilon_d)A_{1z} + \varepsilon_a A_{0x}\cos pz]_{z=\pm L/2} = 0, \tag{15}$$

$$A''_{2z} + \beta^2 A_{2z} = 2k_1k_0A_{1z} - k_a^2A_{1x}A_{0x}\cos pz,$$
$$[(\varepsilon_\perp - \varepsilon_d)A_{2z} + \varepsilon_a A_{1x}\cos pz]_{z=\pm L/2} = 0. \tag{16}$$

Here $\alpha = \sqrt{k_\parallel^2 - k_0^2}$, $\beta = \sqrt{k_\perp^2 - k_0^2}$, $\varkappa_0 = \sqrt{k_0^2 - \omega^2\varepsilon_d/c^2}$.

The solution of system (12) is represented by the two sets of functions

$$A_{0x}^{(n)}(z) = a_\pm^{(n)} f_\pm(\alpha_n z), \qquad \alpha_n = \sqrt{k_\parallel^2 - k_0^{(n)2}}, \tag{17}$$

where $a_\pm^{(n)}$ are constants, $n = 1, 2, 3, \ldots, N$ is the mode number of a *TE*-wave. Here and further in the work the sign "+" corresponds to the mode numbers $n = 2, 4, 6, \ldots$ and function $f_+(x) = \cos x$, and the sign "−" — to numbers $n = 1, 3, 5, \ldots$ and function $f_-(x) = \sin x$. The values of $k_0^{(n)}$ lie in the interval $\omega\sqrt{\varepsilon_d}/c \le k_0^{(n)} \le k_\perp$ and denote the roots of equations $\alpha\sin(\alpha L/2) = \varkappa_0\cos(\alpha L/2)$ and $\alpha\cos(\alpha L2) = -\varkappa_0\sin(\alpha L/2)$ for odd and even n numbers respectively.

In equation (6) we assume $\hat{\varepsilon} = \varepsilon_d\,\hat{1}$ in the medium surrounding NLC ($|z| > L/2$). Using the boundary conditions for the electric field at the NLC surface $z = \pm L/2$, the electric field amplitude of a *TE*-wave in zero approximation with respect to θ_m can be expressed in the following form

$$B_{0x}(z) = e^{\varkappa_{0n}(L/2-|z|)} \begin{cases} a_+^{(n)} \cos(\alpha_n L/2), \\ \operatorname{sign}(z)\, a_-^{(n)} \sin(\alpha_n L/2), \end{cases} \tag{18}$$

where $\varkappa_{0n} = \sqrt{k_0^{(n)2} - \omega^2 \varepsilon_d / c^2}$, $n = 1, 2, 3, \ldots, N$.

Taking into account (17), we obtain the following solution from systems (13) and (16)

$$A_{1x}^{(n)}(z) = 0, \quad k_1^{(n)} = 0, \quad A_{2z}^{(n)}(z) = 0, \quad \text{where } n = 1, 2, 3, \ldots, N. \tag{19}$$

Now the system (15) has the following solution

$$A_{1z}^{(n)}(z) = a_\pm^{(n)} \left[r_{\pm n} f_\pm(\beta_n z) + q_{+n} f_\pm\left((p + \alpha_n) z\right) + q_{-n} f_\pm\left((p - \alpha_n) z\right)\right], \tag{20}$$

where, as follows from the boundary conditions,

$$r_{\pm n} = \frac{1}{2 f_\pm(\beta_n L/2)} \left[\left(\frac{\varepsilon_a}{\varepsilon_d - \varepsilon_\perp} - 2q_{+n} \right) f_\pm\left((p + \alpha_n) L/2\right) + \left(\frac{\varepsilon_a}{\varepsilon_d - \varepsilon_\perp} - 2q_{-n} \right) f_\pm\left((p - \alpha_n) L/2\right) \right],$$

$$q_{\pm n} = \frac{1}{2} \frac{k_a^2}{(p \pm \alpha_n)^2 - \beta_n^2}, \; \beta_n = \sqrt{k_\perp^2 - k_0^{(n)2}}.$$

Substituting the expressions for $A_{0x}^{(n)}(z)$ and $A_{1z}^{(n)}(z)$ into the system (14), we find the function $A_{2x}^{(n)}(z)$ and parameter $k_2^{(n)}$, which are not given here because they take too much space. The unknown components of a *TE*-wave amplitude $\mathbf{B}(z)$ in the dielectric medium outside NLC layer are found in a similar way.

Assuming the intensity of the energy flow along Oy axis (per unit length along Ox) to be 1 W, we find the unknown coefficients $a_\pm^{(n)}$ in (17) with the accuracy up to the small terms of the order of θ_m^2:

$$a_\pm^{(n)} = \frac{4}{c} \sqrt{\frac{\pi \omega}{k_{0n}\left(L \pm \sin \alpha_n L \left(1/\alpha_n + \alpha_n / \varkappa_{0n}^2\right)\right)}}. \tag{21}$$

Thus, the normal *TE*-modes in the dielectric waveguide with a NLC layer are the following

$$\mathbf{E}^{(n)}(y, z) = \mathbf{E}^{(n)}(z)\, e^{ik^{(n)} y}, \qquad n = 1, 2, 3, \ldots, N. \tag{22}$$

The mode amplitudes $\mathbf{E}^{(n)}(z) = (E_{0x}^{(n)}(z) + E_{2x}^{(n)}(z)\theta_m^2,\ 0,\ E_{1z}^{(n)}(z)\theta_m)$ as well as the wave number $k^{(n)} = k_0^{(n)} + k_2^{(n)}\theta_m^2$ are determined by the above formulas (17)–(21), where $\mathbf{E}^{(n)}$ is denoted by $\mathbf{A}^{(n)}$ and $\mathbf{B}^{(n)}$ inside and outside the NLC layer respectively.

The system of equations for coupled modes

We will express the electric field of a *TE*-wave in the dielectric waveguide containing a NLC layer with permittivity tensor $\hat{\varepsilon}(y, z)$ (7) as a superposition of normal modes $\mathbf{E}^{(n)}(y, z)$ (22):

$$\mathbf{E}(y, z) = \sum_{n=1}^{N} C_n(y)\, \mathbf{E}^{(n)}(z)\, e^{ik^{(n)} y}. \tag{23}$$

The coefficients $C_n(y)$ are assumed to be smoothly varying functions at the scale $1/k^{(n)}$. Substituting the solution (23) into the equation (6), which is written in approximation $L \gg \lambda$, we obtain the system of equations for determining the unknown mode amplitudes C_n.

$$C_n' = i\frac{\left|k^{(n)}\right|}{k^{(n)}}\sum_{l=1}^{N}\varkappa_{nl}C_l\left[e^{i\left(k^{(l)}-k^{(n)}+\frac{2\pi}{d}\right)y}+e^{i\left(k^{(l)}-k^{(n)}-\frac{2\pi}{d}\right)y}\right], \quad n=\overline{1,N}. \tag{24}$$

Here the mode coupling coefficient

$$\varkappa_{nl} = \frac{\varepsilon_a \upsilon \omega E_0 \theta_m^2}{32\xi E_\infty \cos\lambda_s}\int_{-L/2}^{L/2}\left[2A_{0x}^{(n)}(z)\,A_{0x}^{(l)}(z)\cos pz - A_{0x}^{(l)}(z)\,A_{1z}^{(n)}(z) - A_{0x}^{(n)}(z)\,A_{1z}^{(l)}(z)\right]\cos(2\lambda_s z/L)\,dz \tag{25}$$

depends on the NLC layer parameters and linear dimensions D and L, external electric field E_0, constant component W_0 and anchoring energy modulation amplitude V as well as the number s (via parameter λ_s) of anchoring energy periods d per NLC length D.

Now we assume the phase-matching condition that is independent of anchoring energy parameters to hold for two modes: number n and l

$$\Delta = k^{(l)} - k^{(n)} - 2\pi/d \ll 2\pi/d. \tag{26}$$

In this case the system (24) acquires the form of Kogelnik's coupled wave equations [29,30] with respect to the amplitudes of these two modes:

$$\begin{cases} C'_n = i\,\text{sign}\left(k^{(n)}\right)\varkappa_{nl}C_l e^{i\Delta y}, \\ C'_l = i\,\text{sign}\left(k^{(l)}\right)\varkappa_{nl}C_n e^{-i\Delta y}. \end{cases} \tag{27}$$

Modes transmission through the NLC layer

We will consider two modes, number n and l, propagating in positive direction along Oy axis. We assume these two modes to satisfy the phase-matching condition (26). The mode with number n is assumed to be a signal-mode whose amplitude at NLC layer boundary $y = 0$ is taken to be $C_n(0) = 0$. The mode with number l is the mode of pumping, which satisfies the condition $C_l(0) = 1$. From the system (27) we find the intensity of the signal-mode at the output of NLC layer in the following form (similar to that in [30]):

$$I = |C_n(D)|^2 = \frac{\varkappa_{nl}^2}{\varkappa_{nl}^2+(\Delta/2)^2}\sin^2\left(\sqrt{\varkappa_{nl}^2+(\Delta/2)^2}D\right), \tag{28}$$

where $\varkappa_{nl}$ and Δ are expressed by formulas (25) and (26) accordingly.

The signal-mode intensity I dependence on the values of D/L-ratio for several values of external electric field E_0 that was calculated by formula (28) in presented in Fig. 3(a). The calculation was performed taking the typical values of the following parameters: elastic constant $K = 10^{-6}$ dyn, waveguide thickness $L = 10\ \mu$m, constant component of anchoring energy $W_0 = 0.06\,\text{erg/cm}^2$ ($\xi = W_0\,L/K = 60$) and the anchoring energy modulation amplitude $\upsilon = V/W_0 = 0.1$. Dielectric constants of NLC were taken for 5CB at the wavelength $\lambda = 615$ nm, and permittivity of the surrounding dielectric medium $\varepsilon_d = 2.1$. The calculations were performed for modes $n = 1$ and $l = 3$, which are the best to meet the phase-matching condition (26) for the given values of above parameters. The dependence of signal-mode intensity I on the length of NLC layer D displays the primary maximum and a number of secondary maxima. The signal-mode intensity I is the largest when $D/L = \tilde{D}_0$,

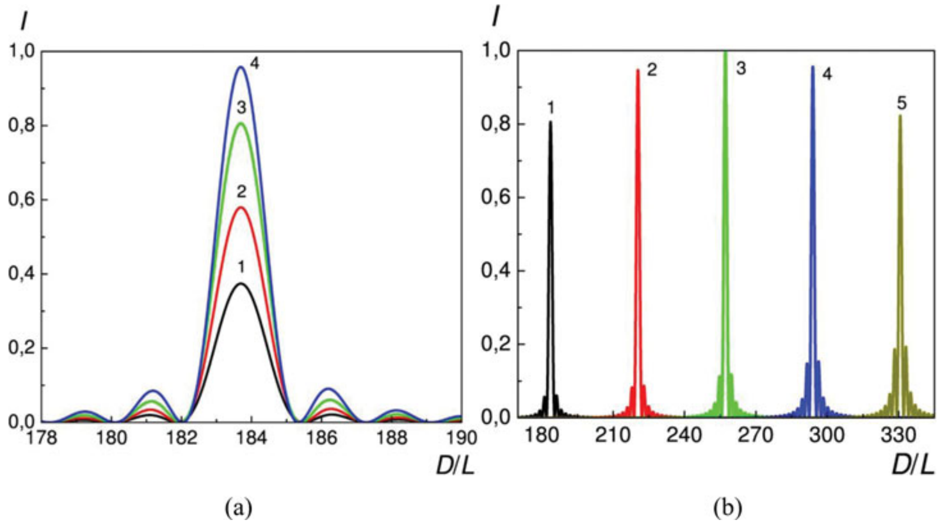

Figure 3. The intensity I of the signal – mode ($n = 1$), where the propagation director is parallel to the pumping mode ($l = 3$), vs. the length of NLC layer D at $\xi = 60$, $\upsilon = 0.1$, $\omega L/c = 102$.(a) $s = D/d = 100$. E_0/E_{0th}= 1.005 (1), 1.007 (2), 1.01 (3), 1.015 (4); (b) $E_0/E_{0th} = 1.01$. s = 100 (1), 120 (2), 140 (3), 160 (4), 180 (5).

which is provided by condition $\Delta = 0$ (see (26)), and equals

$$I_{max} = I\left(\tilde{D}_0\right) = \sin^2\left[\tilde{D}_0\tau\left(\tilde{D}_0\right)\right]. \tag{29}$$

Here

$$\tau(x) = \frac{\sigma\varepsilon_a\omega^2L^2\upsilon}{\gamma c^2\xi}\left(\frac{E_0}{E_{0th}} - 1\right)\frac{E_0}{E_{0th}}\cosh^{-1}\left(\pi\sqrt{(s/x)^2 - 1/4}\right). \tag{30}$$

In (30) σ is the constant which depends on the wave frequency and mode numbers. For the above values of the parameters $\sigma \approx -0.019$.

As seen from Fig. 3(a), the primary maximum of the function $I(D/L)$ increases with growing electric field E_0, and its position (corresponding to $D/L = \tilde{D}_0 \approx 183.7$) remains practically the same. The growth of I_{max} with the increase of E_0 is due to the increase in director grating amplitude (see (5)) and, as a consequence, due to the growth of mode coupling coefficient $\varkappa_{nl}$.

The dependence of signal-mode intensity I on the value of D/L-ratio for fixed external electric field E_0 but for different numbers of anchoring energy periods s per NLC length is presented in Fig. 3(b). When the number s of periods increases, the primary maximum $I_{\max}$ of $I(D)$ shifts steadily towards larger values of D showing, however, non-monotonous change in magnitude in the range from 0 to 1 (according to (29)). The values of the primary maximum I_{max} and corresponding values of D/L- ratio that were calculated as a function of integer s for fixed values of electric field E_0 and anchoring energy parameters ξ and υ are given in Fig. 4(a).

When the amplitude υ grows, the primary maximum $I_{\max}$ of $I(D)$ increases monotonously whereas its position remains the same.

The calculated dependence of signal-mode intensity I on the magnitude of external electric field E_0 for different values of amplitude υ is presented in Fig. 5(a). As seen from the figure, with the increase in E_0/E_{0th}-ratio the intensity I oscillates with a growing amplitude and rapidly, only after a few oscillations, reaches the largest possible value of 1. As the amplitude υ grows, the local maxima of $I(E_0/E_{0th})$ are shifted towards smaller values of E_0/E_{0th}-ratio

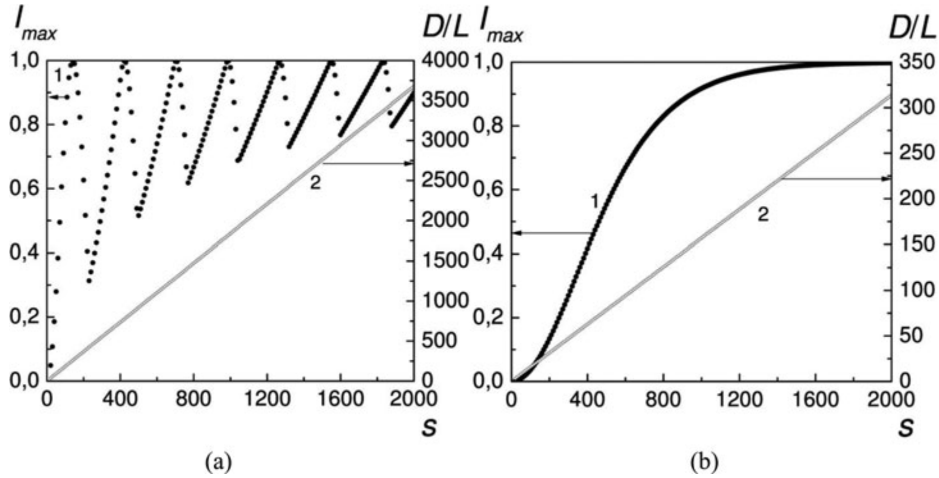

Figure 4. The primary maximum I_{max} (•1) of the signal n – mode, which passes through the NLC layer (a) and reflects from it (b), and corresponding values of D/L – ratio (○2) as functions of integer s at $\xi = 60$, $\upsilon = 0.1$. (a) $n = 1, l = 3, E_0/E_{0th} = 1.01$; (b) $n = l = 1, E_0/E_{0th} = 1.015$.

without changes in magnitude. The fact that local maxima are independent of υ is accounted for by that the director grating amplitude (and, as a result, the coefficient of coupling between the modes) is not determined by the value of the threshold E_{0th} itself (which, according to (5), directly depends on υ) but, instead, by the excess of the threshold value, $(E_0 - E_{0th})/E_{0th}$.

Modes reflection in the NLC layer

Now we consider two modes n and l which propagate in opposite directions. We assume the amplitudes of signal n-mode and l-mode of pumping satisfy the conditions $C_n(D) = 0$, $C_l(0) = 1$ at NLC layer boundaries $y = 0, D$. The signal-mode intensity at the output of the

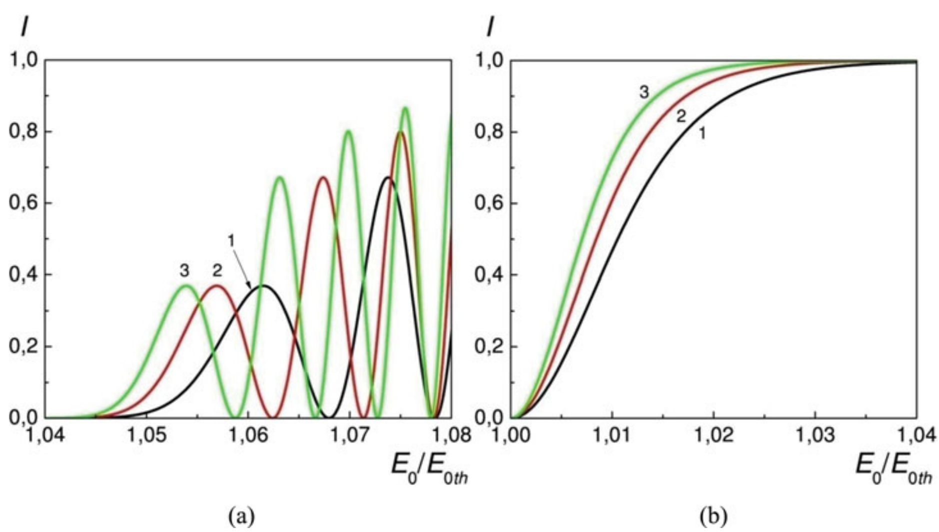

Figure 5. The intensity I of the signal n – mode, which passes through the NLC layer (a) and reflects from it (b), vs. external electric field E_0 at $\xi = 60$. (a) $n = 1, l = 3, D/L = 180, s = 100$. $\upsilon = 0.075$ (1), 0.1 (2), 0.125 (3); (b) $n = l = 1, D/L = 156.9, s = 1000$. $\upsilon = 0.1$ (1), 0.125 (2), 0.15 (3).

NLC layer, which has been found from equations (27), is expressed as in [30]

$$I = |C_n(0)|^2 = \frac{\varkappa_{nl}^2 \sinh^2 \eta_{nl} D}{\eta_{nl}^2 \cosh^2 \eta_{nl} D + (\Delta/2)^2 \sinh^2 \eta_{nl} D}, \quad (31)$$

where $\eta_{nl} = \sqrt{\varkappa_{nl}^2 - (\Delta/2)^2}$, $\varkappa_{nl}$, Δ are given by formulas (25) and (26), respectively.

Let's take the same numbers of the considered modes. In that case we have the mode with a propagation constant $k^{(n)}$ and the mode, reflected from the periodic structure of the NLC layer, with a propagation constant—$k^{(n)}$. Thus, formula (31) determines the intensity I of the reflected n-mode at the NLC layer boundary $y = 0$ (reflectance). For all the values of external electric field E_0, the dependence of the signal-mode intensity I on NLC layer length D is qualitatively analogous to the case of parallel modes (see Fig. 3a): it has the primary and a number of secondary maxima. The primary maximum of the signal-mode intensity I is attained when the phase-matching condition (26) is satisfied at $D/L = \tilde{D}_{c0}$. This has been found to equal

$$I_{c\,max} = \tanh^2 \left[\tilde{D}_{c0} \tau_c \left(\tilde{D}_{c0} \right) \right], \quad (32)$$

where the function $\tau_c(x)$ is obtained from $\tau(x)$, by assuming σ to be approximately equal 1.163×10^8 and function $\cosh^{-1}(\pi\sqrt{(s/x)^2 - 1/4})$ to be substituted by $\cosh^{-1}(\pi s/x)$.

As in the case of transmitted modes, as the value of s grows, the primary maximum position $\tilde{D}_{c0}$ is shifted almost linearly towards greater values of D/L-ratio. However, with the increase in both the number s and anchoring energy modulation amplitude υ the magnitude of the intensity primary maximum I_{max}, according to (32), increases monotonously approaching the maximum value $I_{max} = 1$. The values of the primary maximum I_{max} and respective D/L-ratio calculated as a function of integer s with the fixed values of external electric field and anchoring energy parameters are given in Fig. 4(b). The calculations were performed for the modes with $n = l = 1$ at the wavelength $\lambda = 3785$ nm ($\omega L/c = 16.6$) which are the best to meet the phase-matching condition (26). The electric constants for NLC 5CB at the specified wavelength were taken from [31–33]. As seen from the figure, the intensity primary maximum I_{max} reaches the maximum value $I_{max} = 1$ for $s \gtrsim 1500$.

Unlike the case of transmitted modes, the dependence of reflected mode intensity I on the value of the ratio E_0/E_{0th}, at the fixed values of the amplitude υ, has a qualitatively different character, i.e., it grows monotonously from 0 to 1 (see Fig. 5b). As the amplitude υ increases, the maximum value of reflected mode intensity $I = 1$ is reached at smaller values of the ratio E_0/E_{0th}.

The dependencies of the cutoff frequencies ω_1 and ω_2 of the TE-mode reflection interval on an electric field E_0 are shown on Fig. 6. In the interval $\omega_1 < \omega < \omega_2$ TE-modes reflects from the periodic structure of NLC. TE-modes with frequency $\omega \leq \omega_1$ or $\omega \geq \omega_2$ pass through the NLC layer. As seen from the figure, frequency interval of a TE-mode reflection expands with increasing of an external electric field.

Metal waveguide

Modes transmission through the waveguide

Now we consider an infinitely long planar waveguide with a NLC layer, which is restricted by ideal metal surfaces. The absorption of an electromagnetic TE-wave in both the NLC and metal surfaces bounding the NLC is neglected. The problem is solved analogously to the case of dielectric waveguide, if we take into account the boundary conditions for electromagnetic

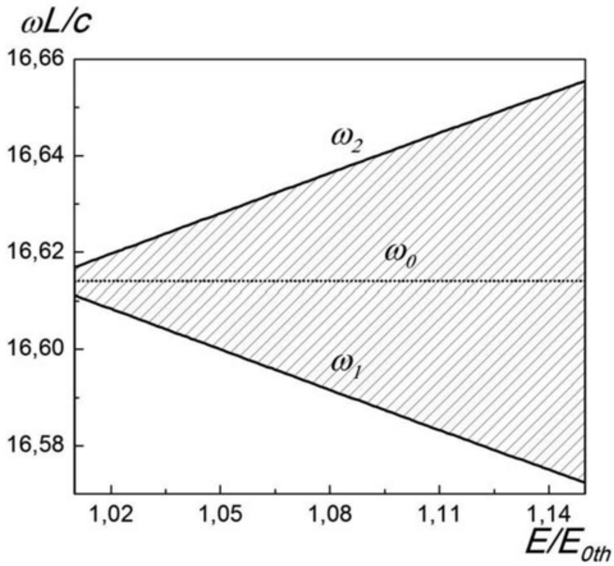

Figure 6. The dependencies of the cutoff frequencies ω_1 and ω_2 of the TE-mode reflection interval $\omega_1 < \omega < \omega_2$ on an electric field. $\omega_0 L/c = 16.6141$ - dimensionless resonant frequency, $\xi = 60$, $s = 1500$, $D/L = 235$, $\upsilon = 0.1$.

field at the metal surface instead of (10). On this condition, the expansion (23) for the electric field of a *TE*-wave in NLC layer will have an infinite number of addends. The intensity of signal n-mode, which is parallel to the pumping l-mode, at the output of NLC layer is expressed by formula (28). The mode coupling coefficient $\varkappa_{nl}$ in this formula is expressed as in (25), where the signs of the two last addends in the subintegral expression have to be changed into their opposites. As previously, the coefficient depends on the length D and the thickness L of the nematic layer, the magnitude of an external electric field E_0, the anchoring energy modulation amplitude υ and the number s of periods of anchoring energy modulation per the length of the NLC layer. The signal-mode intensity I calculated vs. NLC layer length D for fixed external electric field E_0 has turned out to be qualitatively analogous to that for dielectric waveguide given in Fig. 3(a). For D/L-ratio

$$\tilde{D}_0 = 2s\left|\sqrt{\left(\frac{\omega L}{\pi c}\right)^2 \varepsilon_\parallel - l^2} - \sqrt{\left(\frac{\omega L}{\pi c}\right)^2 \varepsilon_\parallel - n^2}\right|^{-1}, \tag{33}$$

corresponding to condition $\Delta = 0$ (see (26)), the signal-mode intensity I has a local maximum whose value is given by expression (29) with the function

$$\tau(x) = -\frac{\frac{\sigma \varepsilon_a \omega L \upsilon}{\gamma c \xi}\left(\frac{E_0}{E_{0th}} - 1\right)\left(1 - \frac{2}{\xi}\right)}{2\left(\frac{s}{x}\right)^2 + 1 - \frac{E_0}{E_{0th}}\left(1 - \frac{2}{\xi}\right)}, \tag{34}$$

where the constant σ is determined by the wavelength and mode numbers. The position $\tilde{D}_0$ of the maximum is independent of the values of the constant component ξ and the amplitude υ.

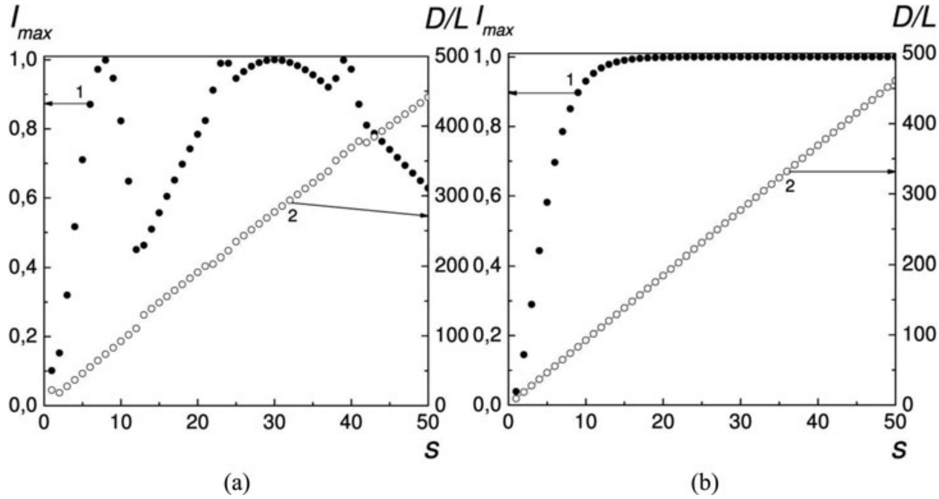

Figure 7. The primary maximum I_{max} (•1) of the signal n – mode, which passes through the NLC layer (a) and reflects from it (b), and corresponding values of D/L – ratio (○2) as functions of integer s. $E_0/E_{0th} = 1.015$, $\xi = 60$, $\upsilon = 0.1$. (a) $n = 5$, $l = 7$; (b) $n = l = 10$.

At points

$$\tilde{D}_m \approx s\left\{\frac{s}{\tilde{D}_0\left(1+\frac{m}{2s}\right)} + \frac{\tilde{D}_0}{\pi^2 m}\tau^2\left[\tilde{D}_0\left(1+\frac{m}{2s}\right)\right]\right\}^{-1} \tag{35}$$

for $m = \pm 2k$, the dependence $I(D/L)$ has local minima that equal zero, and for $m = \pm(2k+1)$—local maxima

$$I_m = I\left(\tilde{D}_m\right) = \frac{\tau^2\left(\tilde{D}_m\right)}{\tau^2\left(\tilde{D}_m\right) + \pi^2 s^2 (1/\tilde{D}_0 - 1/\tilde{D}_m)^2}, \tag{36}$$

where $k = 1, 2, 3, \ldots$. As the number s grows and the amplitude υ decreases, the position $\tilde{D}_m$ (35) of local extremes of $I(D/L)$ dependence are shifted towards greater values of D/L.

The primary maximum I_{max} of the function $I(D/L)$ is attained at one of the points $\tilde{D}_0$ or $\tilde{D}_{+3}$ with a greater value of intensity, $I_{max} = \max\{I_0, I_{+3}\}$.

The values of the primary maximum I_{max} and the respective D/L-ratio calculated as a function of the integer s are given in Fig. 7(a) for fixed values of electric field and anchoring energy parameters ξ and υ. The calculations were performed for the modes $n = 5$ and $l = 7$, which are the best to meet the phase-matching condition (26), and $L = 10\,\mu$m, $\xi = 60$, $\upsilon = 0.1$. Dielectric constants were taken for 5CB at the wavelength $\lambda = 632.8$ nm ($\omega L/c = 100$). The position and magnitude of the primary maximum I_{max} of $I(D/L)$ vary nonmonotonously with the increase both in integer s and the amplitude υ.

For all the values of the amplitude υ the signal-mode intensity I has local extremes in the magnitude of E_0/E_{0th}-ratio at points

$$\tilde{E}_m \approx 1 + 2\left(\frac{1}{\xi} + \frac{s^2 L^2}{D^2}\right)\frac{\sqrt{\frac{\pi^2 m^2 L^2}{4D^2} - \pi^2 s^2\left(\frac{1}{\tilde{D}_0} - \frac{L}{D}\right)^2}}{\sqrt{\frac{\pi^2 m^2 L^2}{4D^2} - \pi^2 s^2\left(\frac{1}{\tilde{D}_0} - \frac{L}{D}\right)^2 + \frac{\sigma \varepsilon_a \omega L \upsilon}{\gamma c \xi}}}. \tag{37}$$

In particular, for $m = 2k$ the minima are equal to zero, and for $m = 2k + 1$ the maxima are equal to

$$I\left(\tilde{E}_m\right) = 1 - \frac{4s^2}{m^2\tilde{D}_0^2}\left(\frac{D}{L} - \tilde{D}_0\right)^2, \tag{38}$$

where $k = 1, 2, 3, \ldots$.

The dependence of signal-mode intensity I on external electric field E_0 has appeared to be analogous to that for dielectric waveguide (see Fig. 5a).

Modes reflection in the waveguide

Now we analyse the reflection of a TE-mode with index n and a propagation constant $k^{(n)}$ from the NLC layer. The intensity of n-mode at the waveguide output is given by formula (31). For all the values of external electric field E_0 the reflected mode intensity I depends qualitatively on D/L analogously to the case of transmitted modes (see Fig. 3a). The primary maximum of reflected mode intensity I_{max} is reached when the value of D/L-ratio is

$$\tilde{D}_{c0} = s\left[\left(\frac{\omega L}{\pi c}\right)^2 \varepsilon_{\parallel} - n^2\right]^{-1/2}, \tag{39}$$

for which the phase-matching condition (26) is met. The magnitude of I_{max} is given by expression (32) for $n = l$ with the function $\tau_c(x) = \tau(x)$ (34). The position of the primary maximum $\tilde{D}_{c0}$ is shifted linearly towards greater values of D/L-ratio with growing s.

At points

$$\tilde{D}_{cm} \approx s\left\{\frac{s}{\tilde{D}_{c0}\left(1 + \frac{m}{2s}\right)} - \frac{\tilde{D}_{c0}}{\pi^2 m}\tau^2\left[\tilde{D}_{c0}\left(1 + \frac{m}{2s}\right)\right]\right\}^{-1}, \tag{40}$$

where function $\tau(x)$ is given by formula (34), $I(D/L)$ dependence has local extremes, in particular, zero minima, for $m = \pm 2k$, and secondary maxima that equal

$$I_{cm} = \left[\frac{\tilde{D}_{c0}\tilde{D}_{cm}\tau\left(\tilde{D}_{cm}\right)}{\pi s\left(\tilde{D}_{cm} - \tilde{D}_{c0}\right)}\right]^2, \tag{41}$$

for $m = \pm(2k + 1)$, where $k = 1, 2, 3, \ldots$.

The values of the primary maximum I_{max} (32) of the reflected mode and corresponding D/L-ratio (39) that were calculated as a function of the integer s at fixed values of electric field and anchoring energy parameters are given in Fig. 7(b). The calculations were performed for the modes $n = l = 10$. Here we take $\omega L/c = 17.97$. The primary maximum of intensity I_{max} monotonously increases with growing number s until the maximum value $I_{max} = 1$ is reached for the values of $s \gtrsim 20$ (almost two orders of magnitude smaller than those for dielectric waveguide).

In contrast to the case of parallel modes, as the external electric field E_0 grows, the reflected mode intensity I increases monotonously from 0 to 1 for all the values of the amplitude υ. In general, the intensity dependence $I(E_0/E_{0th})$ is qualitatively analogous to that presented in Fig. 5(b) for dielectric waveguide. The dependence of the frequency interval of a TE-mode reflection on an electric field E_0 is qualitatively analogous to the case with the dielectric waveguide as well.

Discussion

Controlled by an external low-frequency electric field, the energy exchange between two couple modes of an electromagnetic *TE*-wave at the spatially periodic director grating in the planar NLC waveguide has been theoretically investigated. The director grating emerges when the electric field exceeds the threshold of Freedericksz transition due to the periodicity of the anchoring energy of NLC with waveguide surface. The transmission and reflection of *TE*-modes in both dielectric and metal waveguides have been studied. The intensity of a signal *TE*-mode at the output of the waveguide has been calculated and its dependence on the length D and the thickness L of the nematic layer, the magnitude of an external electric field E_0, the anchoring energy modulation amplitude υ and the integer number s of periods of anchoring energy modulation per the length of the NLC layer has been investigated. The fact that the primary maximum I_{max}, as function of the length D of the nematic layer, increases monotonously with growing electric field E_0 has been established.

The primary maximum of reflected mode intensity I_{max} in both types of waveguides was obtained by selecting an appropriate D/L- ratio, integer number s, number and frequency of the *TE*-mode to satisfy the phase-matching condition (26) best. With increase of the number s and the amplitude υ the primary maximum I_{max} (32) of the dependence $I(D)$ grows monotonously for both types of waveguides. The maximum value $I_{max} = 1$ for the given electric field E_0 is obtained at $s \gtrsim 20$ in the metal waveguide (Fig. 7b) and at $s \gtrsim 1500$ in the dielectric one (Fig. 4b). The increasing of an electric field E_0 results in expanding of frequency interval of a *TE*-mode reflection in the waveguides. The intensity I of the reflected mode monotonously grows from 0 to 1 with the increasing of an electric field E_0 in both types of waveguide.

The magnitude of the primary maximum of transmitted signal-mode intensity I_{max} depends on NLC layer parameters in a more complicated way. For dielectric waveguide the primary maximum I_{max} of signal-mode intensity I as a function of NLC layer length D is attained at those D/L-ratios that satisfy phase-matching condition (26), while in metal one it is found at one of the points, $\tilde{D}_0$ (33) or $\tilde{D}_3$ (35), for which the value of intensity is greater. For both of the waveguides the primary maximum I_{max} of $I(D)$ varies nonmonotonously in the range from 0 to 1 with the increase of the number s. The energy is transmitted to the signal-mode completely only at certain values of D/L-ratio and s number (Figs. 4a and 7a). At higher amplitudes υ the value of the primary maximum I_{max} of $I(D)$ varies monotonously in the dielectric waveguide and non-monotonously in the metal one. The magnitude of D/L-ratio corresponding to the value of I_{max} proves to depend linearly on s number in the dielectric waveguide while in the metal one this dependence is slightly non-monotonous. The dependence of signal-mode intensity I on external electric field E_0 oscillates with growing amplitude. In the metal waveguide the maximum value of signal-mode intensity $I = 1$ is reached at lower E_0/E_{0th}-ratios than in the dielectric waveguide.

The results of the investigation could be used for development and construction of new integrated optical devices. Notice that fact, that the waveguide we have considered, could be used as controllable by an electric field mode-selector for the TE-modes with transmittable frequencies. Thus, one of the TE-modes may subside at the output of the waveguide as a result of a complete conveying its energy to another one. Owing to the complete *TE*-mode reflection for the certain frequency interval, our waveguide could be considered as a controllable by an electric field optical filter. The intensity of the signal-mode at the output of the NLC layer and the width of the frequency interval of a *TE*-mode reflection could be controlled due to varying the amplitude of the spatially periodic refractive index of NLC by an external electric field.

Particularly, the dependences of the primary maximum I_{max} and corresponding ratio D/L on the integer values of s, which are shown in Figs. 4 and 7, for the given electric field and the anchoring energy parameters, allow to select the NLC layer parameters we need.

Acknowledgment

The authors express sincere gratitude to I.P. Pinkevich for useful remarks during the discussion of results.

References

[1] Karpierz, M. A., Domanski, A. W., Sierakowski, M., Swillo, M., & Wolinski, T. R. (1999). *Acta. Physica. Polonica. A*, *95*, 783–792.
[2] Karpierz, M. A., Sierakowski, M., & Wolinski, T. (2002). *Mol. Cryst. Liq. Cryst.*, *375*, 313–320.
[3] Lin, T. S., & Lue, J. T. (2003). *Appl. Phys. B*, *76*, 561–567.
[4] Marangoni, M., Osellame, R., Ramponi, R., Buscaglia, M., & Bellini, T. (2004). *J. Appl. Phys.*, *95*, 5972–5978.
[5] Choudhury, P. K., & Yoshino, T. (2004). *Optik* , *115*, 2, 49–56.
[6] Fratalocchi, A., & Assanto, G. (2005). *Appl. Phys. Lett.*, *86*, 051109, 1–3.
[7] D'Alessandro, A., Asquini, R., Trotta, M., Gilardi, G., Beccherelli, R., & Khoo, I. C. (2010). *Appl. Phys. Lett.*, *97*, 093302, 1–3.
[8] Maksimochkin, A. G., Pasechnik, S. V., Maksimochkin, G. I., & Chigrinov, V. G. (2010). *Opt. Comm.*, *283*, 3136–3141.
[9] Abbate, G., Castaldo, F., De Stefano, L., Mormile, P., Pierattini, G., Righini, G., Santamato, E., & Verciani, A. (1995). *Mol. Cryst. Liq. Cryst.*, *266*, 269–276.
[10] Wiederrecht, G. P., Yoon, B. A., & Wasielewski, M. R. (1995). *Sci.*, *270*, 1794–1797.
[11] Khoo, I. C., Guenther, B. D., Wood, M. V., Chen, P., & Min-Yi Shih. (1997) *Opt. Lett.*, *22*, 1229–1231.
[12] Brignon, A., Bongrand, I., Loiseaux, B., & Huignard, J. P. (1997). *Opt. Lett.*, *22*, 1855–1857.
[13] Ono, H., & Kawatsuki, N. (1999). *J. Appl. Phys.*, *85*, 2482–2487.
[14] Kajzar, F., Bartkiewicz, S., & Miniewicz, A. (1999). *Appl. Phys. Lett.*, *74*, 2924–2926.
[15] Bartkiewicz, S., Matczyszyn, K., Miniewicz, A., & Kajzar, F. (2001). *Opt. Comm.*, *187*, 257–261.
[16] Jones, D. C., & Cook, G. (2004). *Opt. Comm.*, *232*, 399–409.
[17] Pevnyj, M. Ye., Pinkevych, I. P., & Reshetnyak, V. Yu. (2009). *Ukr. J. Phys.*, *54*, 95–100.
[18] Kubytskyi, V. O., Reshetnyak, V. Y., Sluckin, T. J., & Cox, S. J. (2009). *Phys. Rev. E*, *79*, 011703, 1–15.
[19] Reshetnyak, V. Yu., Pinkevych, I. P., Cook, G., Evans, D. R., & Sluckin, T. J. (2010). *Phys. Rev. E*, *81*, 031705, 1–15.
[20] Zografopoulos, D. C., Beccherelli, R. (2013). *J. Opt.*, *15* , 055009, 1–5.
[21] Sugimura, A., & Ishino, D. (2003). *Thin Solid Films*, *438-439*, 433–439.
[22] Cui, Y., Zola, R. S., Yang, Y.-Ch., & Yang, D.-K. (2012). *J. Appl. Phys.*, *11*, 063520, 1–7.
[23] Yeung, F. S. Y., Ho, Y. L. J., Li, Y. W. & Kwok, H. S. (2008). *J. Display Technol.*, *4*(1), 24–27.
[24] Ledney, M. F., & Pinkevich, I. P. (2005). *J. Exp. Theor. Phys.*, *100*, 795–803.
[25] Ledney, M. F., & Tarnavskyy, O. S. (2015). *Crystallography Reports*, *60*, 280–285.
[26] Rapini, A., & Papoular, M. (1969). *J. Phys. (Paris) Collod.*, *30* (Suppl. C4), 54–56.
[27] Ledney M. F., & Tarnavskyy, O. S. (2011). *Ukr. J. Phys.*, *56*, 880–886.
[28] Blinov, L. M., & Chigrinov, V. G. (1994). *Electrooptic Effects in Liquid Crystal Materials*, Springer Verlag, New York, p. 464.
[29] Kogelnik, H. (1969). *Bell Syst. Tech. J.*, *48*, 2909–2947.
[30] Yariv, A., & Yeh, P. (1984). In: *Optical Waves in Crystals*, Goodman, J. W. (Ed.), *Wiley Series in Pure and Applied Optics*, Wiley, New York, p. 589.
[31] Jun, Li. & Shin-Tson, Wu. (2004). *J. Appl. Phys.*, *95*, 3,896–901.
[32] Li, J., & Wu, S.-T. (2004). *J. Appl. Phys.*, *96*, 1, 170–174.
[33] Tkachenko, V., Abbate, G., et al. (2006). *Mol. Cryst. Liq. Cryst.*, *454*, 263/[665]–271/[673].